Digest Journal of Nanomaterials and Biostructures Vol. 8, No. 1, January - March 2013, p. 207 - 217

ADSORPTION AND RELEASE OF STRONTIUM FROM HYDROXYAPATITE CRYSTALS DEVELOPED IN SIMULATED BODY FLUID (SBF) ON POLY (2-hydroxyethyl) METHACRYLATE SUBSTRATES

J. BEUVELOT[a], Y. MAURAS[b], G. MABILLEAU[a], H. MARCHAND-LIBOUBAN[a], DANIEL CHAPPARD[a*]

[a]*LUNAM Université, GEROM- LHEA « Bone Remodeling and bioMaterials » – IRIS-IBS Institut de Biologie en Santé, CHU d'Angers, 49933 ANGERS Cedex - FRANCE.*

[b]*Laboratoire de Pharmacologie, CHU d'Angers, 49933 ANGERS Cédex - FRANCE.*

Poly (2-hydroxy ethyl) methacrylate (PHEMA) is a polymer that can be carboxymethylated to induce calcification on its surface. This mimics the calcification of bone matrix since the polymer surface induces the deposit of large hydroxyapatite calcospherites. We investigated the effect of Sr^{2+} on hydroxyapatite crystals developed on PHEMA pellets. Pellets were incubated for 1 week in a synthetic body fluid (SBF) to induce mineralization, then 2 weeks in SBF containing 0, 130, 260 or 390 µM of Sr^{2+} allowing growth and maturation of calcospherites. Calcospherites were dissolved in HCl and Ca^{2+}, PO_4^{3-} and Sr^{2+} content was measured. Sr^{2+} release was assessed by transferring other pellets in saline which was collected at regular intervals to measure Sr^{2+} release. Hydroxyapatite was characterized by SEM, X-ray diffraction, FTIR and Raman microspectroscopy. After the maturation period, Sr^{2+} was incorporated into hydroxyapatite crystals as a function of its concentration in SBF. However, size of the calcospherites decreased as a function of the strontium concentration. During the release phase, the slope of Sr^{2+} elution was progressive and similar independently of the initial concentration; ~30% Sr^{2+} was released after 61 days. XRD showed that incorporation of Sr^{2+} produced no significant change in crystal lattice parameters or cristallinity. A progressive release of Sr^{2+}occurred from the crystals. Strontium can be adsorbed rapidly on hydroxyapatite crystals and can be released easily. Carboxymethylated PHEMA can be used to study the effect of chemical compounds on the growth of hydroxyapatite nodules and their release in a second time.

(Received November 9, 2012; Accepted January 7, 2013)

Keywords: Strontium; Hydroxyapatite; Mineralization; Release; Poly (2-hydroxyethyl) methacrylate.

1. Introduction

Poly (2-hydroxyethyl methacrylate) (PHEMA) has been extensively used as a biomaterial with potentially wide applications such as contact or intraocular lenses, soft-tissue replacement, contraceptive techniques or vascular prostheses (see review in Monthéard et al. [1]). It can be prepared in various forms including porous scaffolds [2]. We previously reported that carboxymethylation of PHEMA (CM-PHEMA) produded a polymer that can mimic the calcification of woven bone [3]. By using this polymer, it is possible to evaluate the growth of hydroxyapatite in presence of ions or compounds that can interfere with calcification [4, 5]. Strontium (Sr^{2+}) is an antiosteoporotic agent having a dual effect on bone remodeling: it acts by

* Corresponding author: daniel.chappard@univ-angers.fr

decreasing bone resorption while increasing bone formation [6, 7]. This effect is responsible for the Sr^{2+} efficacy in the treatment of postmenopausal osteoporosis [8]. Due to its osteogenic properties, several recent attempts have been done to incorporate Sr^{2+} in various biomaterials since it can improve osseointegration [9-13].

Sr^{2+} is also a metallic cation that can be trapped in the hydroxyapatite crystals (HAP) of the bone matrix by adsorption onto the crystal or by substitution of Ca^{2+} ions [14, 15]. However, recent clinical data indicate that Sr^{2+} is loosely bound to HAP crystals of the bone matrix by ionic substitutions and easily exchangeable from bone mineral [16]. This tends to indicate a weak binding of Sr^{2+} onto the outer shell of the crystal rather than a substitution of Ca^{2+} by Sr^{2+} in the depth of the crystals.

The aims of the present study were (1) to evaluate the effect of strontium on the hydroxyapatite crystals development in an *in vitro* model of calcification based on pellets of CM-PHEMA [3]. Pellets of the polymer were incubated in a synthetic body fluid containing Sr^{2+} at increasing concentrations. The effects of Sr^{2+} incorporation on crystal growth, crystallinity and crystallographic characteristics were investigated. (2) To test the clearance of Sr^{2+} from the HAP crystals that have grown in these strontium rich media by transferring the pellets in saline devoid of Sr^{2+}.

2. Material and methods

2.1 Preparation of pellets of carboxylated polymer

Commercial 2-hydroxyethyl methacrylate (HEMA) (Aldrich Chemical, Illkirsh, France) contains residual methacrylic acid and EGDMA because of the fabrication process. The polymerization inhibitor 4-methoxyphenol (added by the manufacturer before shipping, at a concentration of 350 ppm) also needs to be removed. HEMA was purified and distilled under reduced pressure (5×10^{-2} mbar, 50°C).

Polymer was prepared by bulk polymerization. The polymerization mixture was composed of HEMA (10mL) and benzoyl peroxide 0.2g used as initiator. The mixture was accelerated by N,N-dimethyl-para-toluidine in a 100:1 (mol/mol) ratio of initiator to accelerator. The monomer was polymerized at 4°C for 2h in polypropylene wells (Delta Microscopies, Labege, France) to obtain calibrated pellets of PHEMA as previously described [3, 4]. Pellets were carboxymethylated by soaking in 0.5M bromoacetic acid in a 2M NaOH solution during 24h at room temperature, under gentle agitation. Pellets of the CM-PHEMA were washed 3 times (10 minutes each) in deionized water and dried in an oven at 40°C. They were sterilized by UV radiation (360 nm for 3 hours) before use. The success of carboxymethylation of the biomaterial was assessed by Fourier Transformed Infra-Red (FTIR) measurement. Infrared spectra in the range of 950–4000cm^{-1} were recorded at 32 scans per spectrum at 8cm^{-1} resolution using a Bruker Hyperion 3000 rapid microscope (Brukers optics, Germany) equipped with a single element Mercury Cadmium Telluride (MCT) detector.

2.2 Incubation of pellets in synthetic body fluid (SBF)

A standard synthetic body fluid (SBF) mimicking the extracellular fluids was prepared according to Yamada and al [17]. Its composition was as follows: Na^+: 171.25 mM; Ca^{2+}: 3.11 mM; Mg^{2+}: 1.87 mM; HCO_3^-: 5.25 mM; Cl^-: 172.5 mM; HPO_4^-: 1.12 mM; SO_4^2: 0.62 mM; K^+: 4.85 mM. The medium was supplemented with penicillin (100 UI/ml) and streptomycin (500 µg/ml) to avoid mould and bacterial contamination. The rheogram of the study appears on Figure 1. Pellets of CM-PHEMA biomaterials were distributed in sterile capped vials containing 50 mL of the synthetic medium at 37°C. The calcification of the pellets was initiated during 1 week without adding of Sr^{2+}. After this period, the development of HAP calcospherites took place during 14 days in SBF containing 0, 130, 260 and 390 µmol/L of Sr^{2+}. The media were changed every 2 or 3 days. These concentrations corresponds to 1x, 2x and 3x values of Sr^{2+} reached in the serum of patients receiving a Sr^{2+} for the treatment of post-menopausal osteoporosis [18].

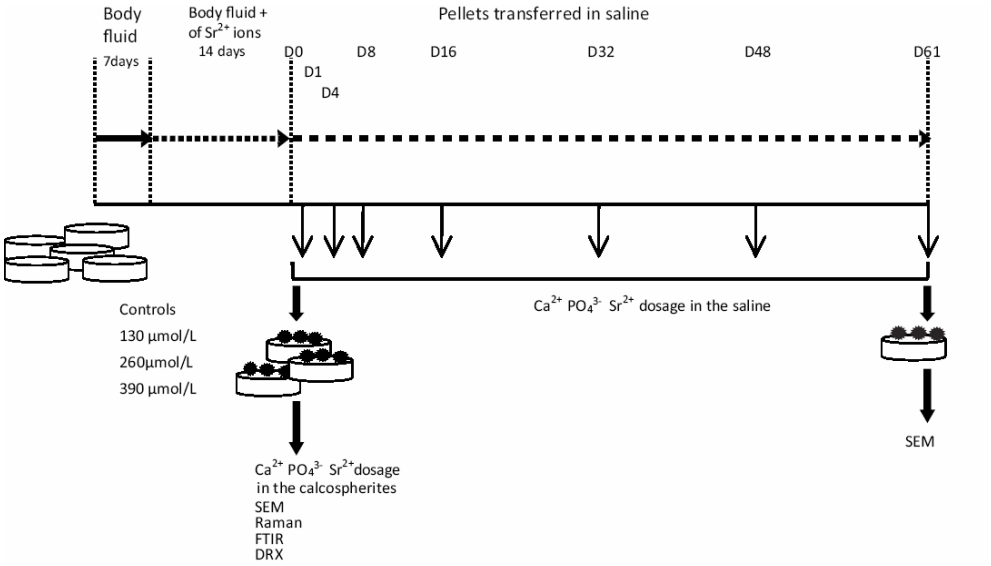

Fig. 1. Flow chart of the study. Pellets of CM-pHEMA were immersed in SBF during 1 week to initiate calcification, then Sr^{2+} ions were added during 2 weeks in the SBF (3 different concentrations). One part of the pellets was analyzed and others were used for Sr^{2+} elution. Saline was analyzed at day 1, 4, 8, 16, 32, 48 and 61. At day 61, pellets were dried and analyzed for calcospherite morphology and composition.

2.3 Scanning electron microscopy analysis (SEM)

SEM observation of pellets covered by calcospherites was performed on a JEOL 6301F (JEOL, Tokyo, Japan) field emission microscope with an accelerating 5 kV voltage at a distance of 15 mm. The microscope is equipped with an energy dispersive X-ray micro-analysis machine (EDX; Link ISIS, Oxford Instruments, Oxford, UK). Ten pictures per pellets were taken at a magnification of 4000x without tilt and 20 calcospherites per image to were measured the size of calcospherites with the ImageJ 1.34s software (NIH). SEM analysis was performed on 3 pellets per group.

2.4 Chemical analysis

At the end of the mineralization period, pellets incubated with either 0, 130, 260 and 390 µmol/L Sr^{2+} were rinsed in deionized water for 3 x 10 minutes to remove the non-crystallized ions. Transfer of the pellets in HCl 0.2M (2 mL) for 24 hours led to a complete dissolution of calcium/phosphate crystals. Calcium was dosed on a Modular spectrometer (Roche diagnostics, Meylan, France) by colorimetry with cresol phtaleine complexon and phosphate was dosed by colorimetry with ammonium phosphomolybdate. Sr^{2+} was dosed by inductively coupled plasma atomic emission spectrometry (ICP-AES) on a Jobin Yvon JY 238 Ultrace (HORIBA JOBIN-YVON, Longjumeau, France). Each measure was performed on 3 pellets/group.

2.5 FTIR analysis

For each incubation condition, 3 additional mineralized pellets were dried in an oven during 24h at 37 °C. Fourier Transformed Infra-Red (FTIR) analysis was performed to characterize the calcospherites formed on the PHEMA substrates. Spectra in a range of 950-4000cm^{-1} were recorded at 32 scans per spectrum at 8cm-1 resolution using a Bruker Hyperion 3000 scan microscope (Bruker) with a single element Mercury Cadmium Telluride (MCT) detector. Infrared spectra were recorded in the reflexion mode. A background spectrum was collected, containing data from the environment, the instrument and the optical discs. Dried mineralized PHEMA pellets were disposed on the spectrometer and spectra were done on 3

samples from each Sr^{2+} concentration. Five different areas were analyzed on each sample and a mean spectrum was obtained for each concentration with the Bruker's proprietary Opus Software (release 5.5).

2.6 Raman analysis

Raman microspectroscopy was performed on a Senterra microscope (Bruker Optik, also working with the Opus software) on 3 additional pellets in each incubation condition. The excitation laser wavelength was 785 nm. The long working distance of the 20x microscope objective gave a spot size in the order of 2 µm. Automatic baseline correction removed residual fluorescent background, resulting in fluorescence-free spectra. Dried mineralized PHEMA pellets were disposed on the spectrometer and spectra were done on 3 samples prepared with 0, 130, 260 and 390 µmol/L of Sr^{2+} concentrations. Five different areas were analyzed on each sample and a mean spectrum was realized for each concentration.

2.7 X-ray diffraction (XRD)

X-ray diffraction was used to characterize mineral deposits on 3 pellets in each incubation condition. Dried mineralized pellets were rapidly moistened with water and pressed under a pressure of 2 bars to obtain a very flat sample. Flat pellets were placed onto a metallic support and examined with a D8 X-ray diffractometer with Cu Kα cathode (Brucker, France). The spectra were recorded at room temperature between 20 and 56° corresponding to 2θ and a measure was performed every 0.02°. Parameters a and c of the crystal unit cell were calculated [19].

2.8 Strontium release measurement

Another group of biomaterial pellets was used to study the release of Sr^{2+}. Once the pellets have been incubated with SBF enriched in Sr^{2+}, they were rapidly rinsed in saline to remove the non-crystallized ions and placed in sterile tubes containing 2mL of saline. Tubes were gently agitated at 37 °C, supernatants were collected and the medium was replaced after 1, 4, 8, 16, 32, 48 and 61 days. Dosages of Sr^{2+}, Ca^{2+} and PO_4^{3-}, released in saline at these time points, were done as described above. Four pellets were incubated for each period and the analysis was done in duplicate. The amount of residual Sr^{2+} in the pellets was derived from the dosages and expressed as the percentage of the value obtained on the dissolved calcospherites at D0 which represented the 100% amount of Sr^{2+} adsorbed for each dosage.

2.9 Statistical analysis

Statistical analysis was performed with Systat 13 statistical software (Systat Software, Inc., San José, CA). All data were reported as mean ± standard error of the mean (SEM). The frequency distribution of calcospherite's size for each sample was assessed; if the distribution was lognormal, data were converted to logarithmic values and differences between groups were analyzed by ANOVA with a post-hoc test (Fisher's least significant difference). Differences were considered as significant at $p < 0.05$.

3. Results

3.1 Calcification of PHEMA pellets

After one week of incubation, SEM showed the formation of nodules on the CM-PHEMA surface (Figure 2). Mineralized nodules had a rounded shape (calcospherites) and were made of elementary tablets, or plates of HAP, packed together.

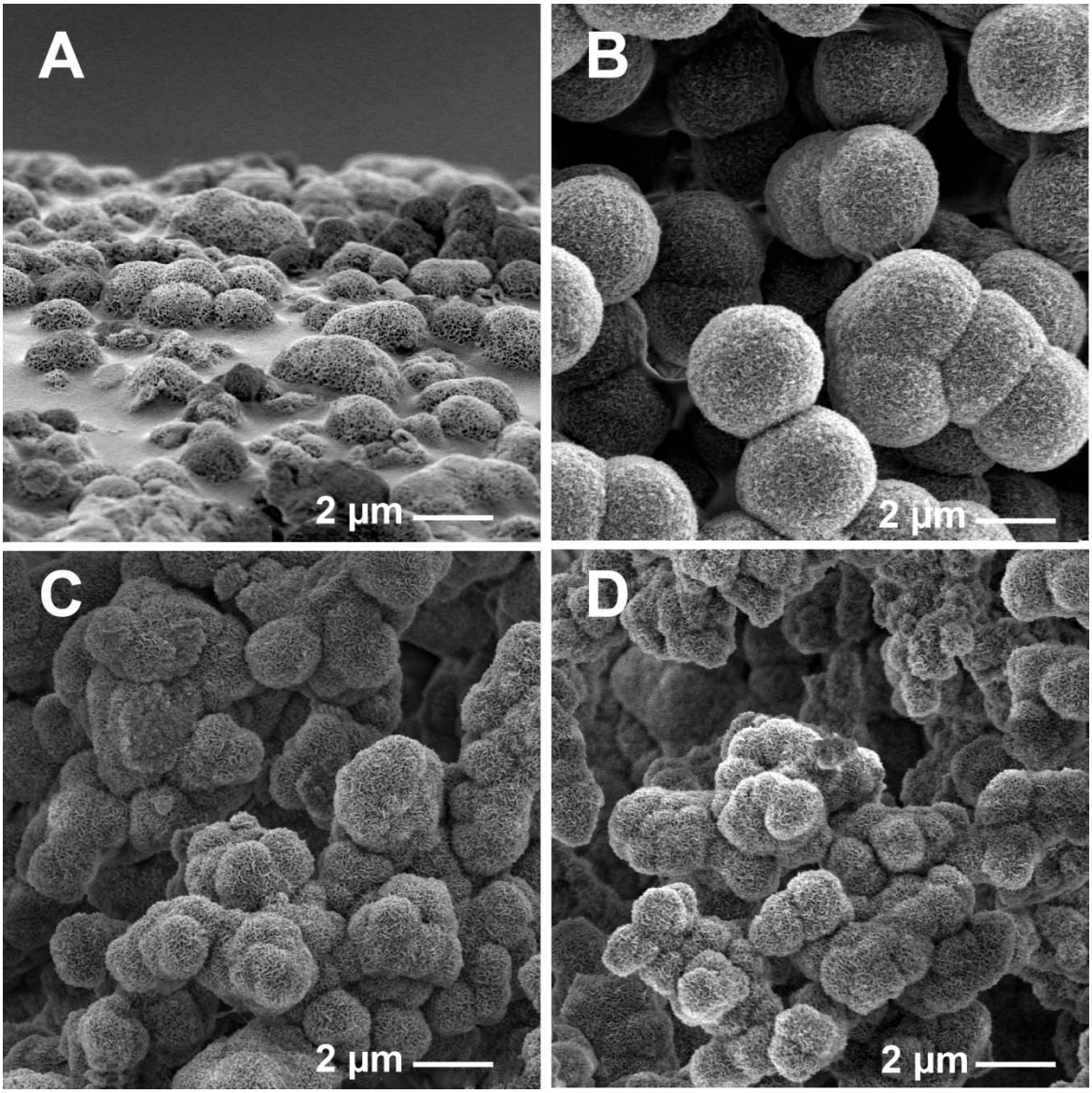

Fig. 2. Calcospherite formation and growth at the biomaterial surface. A) the growth of calcospherites starts at the surface of the polymer which induces the deposit of HA crystals. The image is tilted to better illustrate the HA induction from the biomaterial itself; B) calcospherites grown in the absence of Sr^{2+} ions during 2 weeks; C) calcospherites grown in the presence of 260 µmol/L of Sr^{2+} ions during 2 weeks have a reduced size; D) calcospherites grown in the presence of 390 µmol/L of Sr^{2+} ions during 2 weeks have a more reduced size.

After 2 weeks of incubation in presence of Sr^{2+} in the SBF, the size of calcospherites decreased slightly but significantly when Sr^{2+} concentration increased. Calcospherites were significantly smaller in SBF with 260 and 390 µmol/L of Sr^{2+} than with 130 µmol/L (Figure 3).

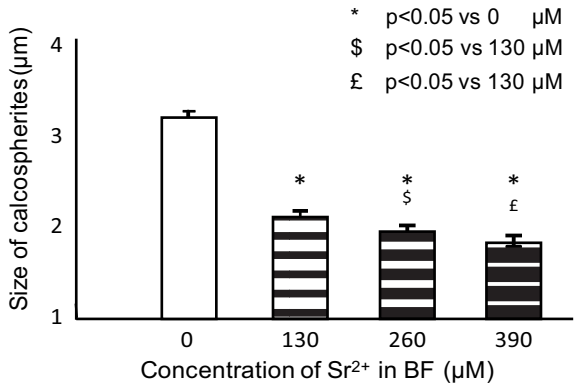

Fig. 3. Calcospherite diameter and Sr^{2+} concentrations in body fluid. With increasing Sr^{2+} concentration, calcospherite decreased slightly in diameter.

3.2 Chemical analysis

Sr^{2+}, Ca^{2+} and PO_4^{3-} concentrations in mineral appear on Fig. 4. The amount of Sr^{2+} fixed in the calcospherites significantly mirrored the concentration of Sr^{2+} in SBF. A negligible amount of Sr^{2+} was detected in calcospherites formed in SBF without Sr^{2+}, corresponding to the resolution of the dosage method. Ca^{2+} and PO_4^{3-} contents in calcospherites did not vary when Sr^{2+} concentration increased in SBF.

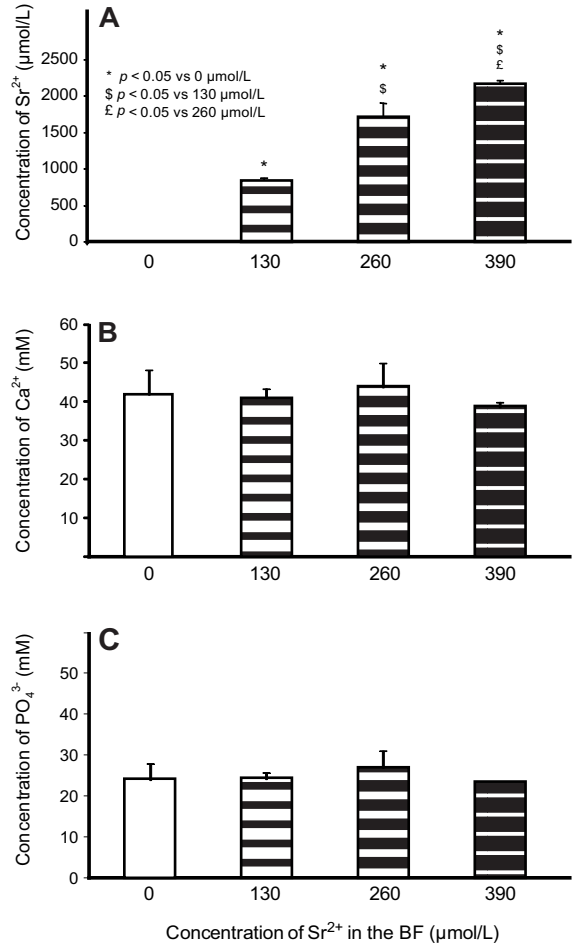

Fig. 4. Amounts of (A) Sr^{2+}, (B) calcium and (C) phosphate measured in the calcospherites after the incubation period. The Sr^{2+} amount increased with the Sr^{2+} concentration in SBF whereas calcium and phosphate did not vary.

3.3 FTIR analysis

All FTIR spectra of dried pellets were similar (Fig. 5): independently of the concentration of Sr^{2+} in SBF, a broad peak of ν3 PO_4 was observed at 1150 cm^{-1} and a weaker peak at 960 cm^{-1}, representing ν1 PO_4 [20]. All spectra showed peaks at 1470 and 880 cm^{-1}, corresponding to stretching vibrations of CO_3^{2-}. The peak observed at 1750 cm^{-1} was affected to the –COOH function which came from the carboxymethylation of the pellets.

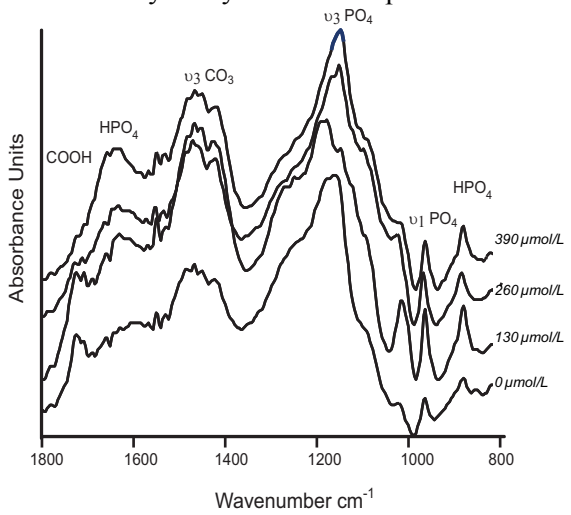

Fig. 5. Infra-red spectra of mineralized pellets after incubation in SBF. Broad peak of υ3 PO_4^{3-} was observed at 1150 cm^{-1} and a weaker peak at 960 cm^{-1}, representing υ1 PO_4^{3-}. All spectra showed peaks at 1470 and 880 cm^{-1}, corresponding to stretching vibrations of CO_3^{2-}.

3.4 Raman analysis

On the raman spectra (Figure 6), ν1, ν2, ν4 and ν3 of PO_4^{3-} were observed respectively at 960 cm^{-1}, 400-500 cm^{-1}, 550- 650 cm^{-1} and 1000-1100 cm^{-1}. [21-23]. All spectra presented the ν2 band of CO_3^{2-} at 879 cm^{-1}. This peak was overimposed on the HPO_4^{2-} peak [24].

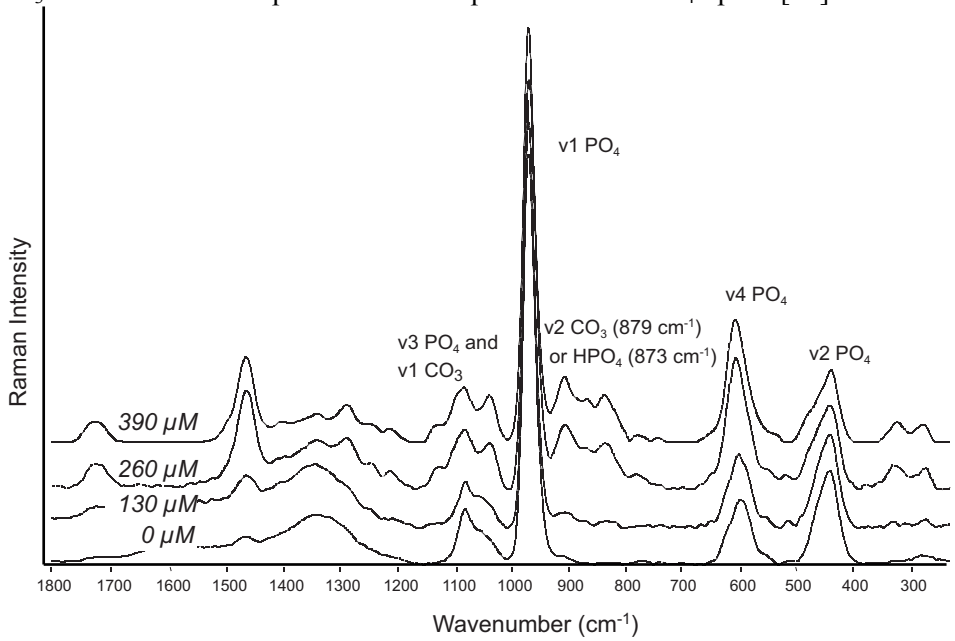

Fig. 6. Raman spectra obtained from pellets incubated in presence of 0, 130, 260 and 390 µmo/L of Sr^{2+}. Note the appearance of the peak at 960 cm^{-1} corresponding to the υ1 PO_4^{3-} of HAP.

3.5 X-ray diffraction

Table 1 showed the variation of a and c crystal parameters with the Sr^{2+} concentrations in SBF. The lengths of the *a* and *c* axis did not vary significantly in the presence of various concentrations of Sr^{2+} in SBF.

Table 1 : Variations of crystal parameters a and c as function of the Sr^{2+} concentration in BF and of Sr^{2+} quantity integrated in calcospherites.

Sr^{2+} concentration in BF (µM)	Sr^{2+}/Ca^{2+} (% integrated in mineral)	Cristal Parameter *c* (Å)	Cristal Parameter *a* (Å)
0	0.0032 ± 0.0001	6.848 ± 0.03	9.654 ± 0.053
130	2.1 ± 0.3	6.833 ± 0.006	9.610 ± 0.009
260	4.0 ± 0.1	6.846 ±0.066	9.616 ±0.092
390	5.61 ± 0.09	6.862 ± 0.019	9.652 ±0.033

3.6 Release of Sr^{2+}

Independently of the Sr^{2+} concentration used in SBF during growth of the calcospherites, the curves describing the release of Sr^{2+} presented with the same shape (Figure 7). Until day 4, the release of Sr^{2+} was important, approximately around 20% of the total incorporated Sr^{2+}. Then, the slope of the curve was slower and a 30% release of total Sr^{2+} was obtained after 61 days. The SEM analysis of the pellets at the end of the release period did not revealed any change when compared to those at D0.

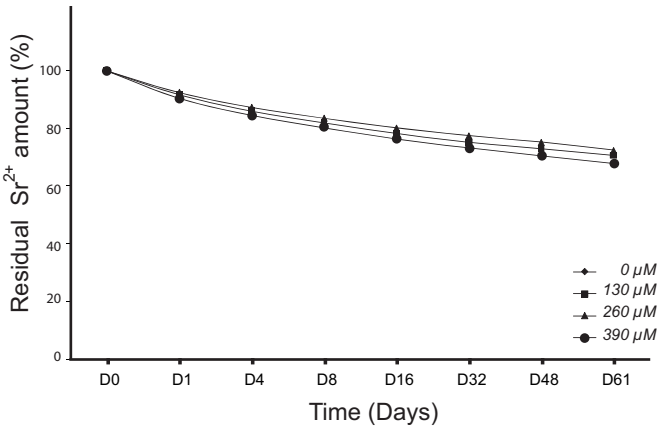

Fig. 7. Sr^{2+} desorption from the calcospherites up to 61 days. After 8 days, ~20% of the incorporated Sr^{2+} was eluted, at 61 days: ~30%.

4. Discussion

Our work aimed to observe the effect of Sr^{2+} on the formation of hydroxyapatite grown on a synthetic polymer, CM-PHEMA, which constitutes an *in vitro* system that do not imply cell or protein intervention in a biomimetic approach. HAP is the main phase of the bone mineral and is often used as a bone filling biomaterial. Carboxymethylation of a polymer is sufficient to initiate HAP nucleation and calcospherites deposition [3]. Carboxylic groups can attract Ca^{2+} cations and initiate calcium-phosphate precipitation into HAP. This materials reproduces the effects of

biological molecules such as the bone sialoprotein (BSP) known to induce bone nucleation *in vivo* [25]. This *in vitro* model has been extensively used to characterize the effect of pharmacological drugs, metallic ions or proteins known to interfere with bone calcification [4, 5, 26, 27]. In this study, CM-PHEMA pellets were used to induce the development of calcospherites when incubated in SBF and FTIR and EDX assessments confirmed they were made of HAP. The polymer itself does not contains ions that participate in the calcification process.

In vivo, amounts of Sr^{2+} in the bone structure units vary at the end of the treatment according to the bone site [28]. In addition, it has been shown that Sr^{2+} is dose-dependently taken up by the mineral phase of the bone matrix [16]. One Sr^{2+} ion is incorporated for 10 Ca^{2+} in the crystal lattice [29]. In this study, Sr^{2+} incorporation into the calcospherites increased as a function of its concentration in SBF. The calcospherites formed were similar in shape and size to those formed *in vivo* in human woven bone [26]. However, significant differences in the mean calcospherite diameter is difficult to explain from this experiment other than by complex thermodynamic changes. Similarly, it was reported that $CaCO_3$ crystals form complex aggregates with different size that differ thermodynamically when small amounts of ethanol are added [30]. Incorporation of Sr^{2+} in HAP did not affect the crystal parameters as shown by others with *in vitro* studies excepted when considerable amount of Sr^{2+} are used to prepare synthetic ceramics [31-33]. In a monkey study, variations of parameters *a* and *c* were not significant between control and animals receiving a 13-week treatment with high doses of strontium [16]. Comparisons were made between Sr^{2+} incorporation in the rat, monkey and human bones; it was shown that, independently of the dose administered, Sr^{2+} incorporation in bone did not affect the crystal lattice parameters even if the ionic radius of Sr^{2+} is higher than that of Ca^{2+} (0.113 *vs* 0.099 nm) [16, 19, 28, 34, 35]. In addition, thickness and length of the plate-shaped bone mineral crystals were not affected by the strontium treatment in a human study [36]. In our study, values measured for *a* and *c* parameters were very close to those reported for bone mineral ($a = b = 0.9432$ and $c = 0.6881$ nm), independently of the concentration of Sr^{2+} used in SBF [37]. Furthermore, Sr^{2+} incorporation onto the calcospherites did not affect cristallinity, independently of the concentration of Sr^{2+} in SBF. Howeve, the mean diameter of the calcospherites decreased as a function of Sr^{2+} concentration in the SBF. This finding is not contradictory with previous results since the thermodynamic characteristics of the calcospherites are largely unknown. The nucleation and gowth forms of polycrystalline structures can be altered by external factors even if each crystal is not affected [38]. We have previously reported that proteins such as fetuin and osteocalcin could modify considerably the size of calcospherites by controlling the nucleation of hydroxyapatite [27].

The present study was also designed to study the release of Sr^{2+} from the mineral since no report have looked at the release of this ion from a strontium-containing biomaterial. We found that 30% of the total incorporated Sr^{2+} was released after 61 days. *In vivo* studies done on monkeys have shown a rapid release of Sr^{2+} after treatment discontinuation [19]. The animals had received a one year treatment with a Sr^{2+} salt and 10 weeks after the cessation of the treatment, the Sr^{2+} content int the iliac crest bone was decreased by 50% when measured by X-ray microanalysis and quantitative microradiography. In one arm of the SOTI study concerning the treatment of osteoporotic patients with a Sr^{2+} salt (Sr ranelate), the drug was discontinued after 4 years while other patients were treated during a 5^{th} year. A significant decrease of mineral density progressively occurred in the untreated arm as a consequence of Sr^{2+} elimination. The spontaneous release of Sr^{2+} occurred and followed a typical elution curve. However, the results markedly differ from those obtained in *in vivo* studies which indicate that much more Sr^{2+} is released. This can be explained by considering that our *in vitro* model did not take into account a possible exchangeable pool of strontium linked to proteins and that no cellular event is present *in vitro*. Sr^{2+} release from the calcospherites grown on CM-PHEMA pellets indicated that this element was weakly linked to crystals by ionic substitution. This reflect what can happen in vivo when grafting HAP enriched in Sr^{2+}. However, it is likely that bone remodeling and the *in vivo* environment accelerate the Sr^{2+} release by additional mechanisms such as matrix (or biomaterial) resorption by osteoclasts (bone resorbing cells). The present study has also confirmed by X-ray analysis that the uptake of Sr^{2+} preserved HAP crystallinity and characteristics of crystal units. These findings corroborate

previous studies suggesting that Sr^{2+} is mainly incorporated by ion exchange onto the crystal surface and can be released upon time.

5. Conclusion

CM-PHEMA represents an easy method for the study of interactions of pharmacological compounds, ions or biological molecules that can interfere with the calcification process. With this method, we report that the amount of Sr^{2+} deposited in the HAP crystals developped on the CM-PHEMA biomaterial is a function of the initial concentration in the body fluid. The crystallinity was unchanged independently of the intital concentration of Sr^{2+}. A progressive release of Sr^{2+} occurred by spontaneous release from the crystals. These findings demonstrated a possible mechanism to explain Sr^{2+} release from the bone matrix and how this element might exert its osteogenic action. This also confirms that HAP-based biomaterials containing Sr^{2+} can release the active ion progressively in the microenvironment of the graft.

Acknowledgments

This work was made possible by grants from Contrat de Plan Etat – Région "Pays de la Loire" Bioregos2 and IRIS. Thanks to Mrs. L. Lechat for secretarial assistance. SEM analyses were performed at Service Commun d'Imagerie et d'Analyses Microscopiques (SCIAM), Université d'Angers with many thanks to Romain Mallet. DRX analyses were performed at CIMA Laboratory, Université d'Angers with Magali Allain. Ion measurements were performed at the Pharmacology and Biochemistry Laboratories - CHU of Angers.

References

[1] J. P. Monthéard, M. Chatzopoulos, D. Chappard, J. Macromol. Sci. Rev. Macromol. Chem. Phys. **C32** 1 (1992).
[2] I. C. Stancu, P. Layrolle, H. Libouban, R. Filmon, G. Legeay, C. Cincu, M. F. Baslé, D. Chappard, J. Optoelectron. Adv. Mater. **9** 2125 (2007).
[3] R. Filmon, F. Grizon, M. F. Baslé, D. Chappard, Biomaterials **23** 3053 (2002).
[4] P. Guggenbuhl, R. Filmon, G. Mabilleau, M. F. Baslé, D. Chappard, Metabolism. **57,** 903 (2008).
[5] G. Mabilleau, R. Filmon, P. K. Petrov, M. F. Baslé, A. Sabokbar, D. Chappard, Acta Biomater. **6** 1555 (2010).
[6] P. J. Marie, Curr. Opin. Rheumatol. **18 S1** S11 (2006).
[7] P. J. Marie, D. Felsenberg, M. L. Brandi, Osteoporos. Int. 1 (2010).
[8] J. Y. Reginster, E. Seeman, M. C. De Vernejoul, S. Adami, J. Compston, C. Phenekos, J. P. Devogelaer, M. D. Curiel, A. Sawicki, S. Goemaere, O. H. Sorensen, D. Felsenberg, P. J. Meunier, J. Clin. Endocrinol. Metab. **90** 2816 (2005).
[9] B. Busse, B. Jobke, M. Hahn, M. Priemel, M. Niecke, S. Seitz, J. Zustin, J. Semler, M. Amling, Acta Biomater. **6** 4513 (2010).
[10] P. Kanchana, C. Sekar, J. Appl. Biomater. Biomech. **8** 153 (2010).
[11] W. Zhang, Y. Shen, H. Pan, K. Lin, X. Liu, B. W. Darvell, W. W. Lu, J. Chang, L. Deng, D. Wang, W. Huang, Acta Biomater. **7** 800 (2011).
[12] Y. Li, Q. Li, S. Zhu, E. Luo, J. Li, G. Feng, Y. Liao, J. Hu, Biomaterials **31** 9006 (2010).
[13] L. Maimoun, T. C. Brennan, I. Badoud, V. Dubois-Ferrière, R. Rizzoli, P. Ammann, Bone **46** 1436 (2010).
[14] G. Boivin, P. J. Meunier, Osteoporos. Int. **14 S3** S19 (2003).
[15] S. Pors Nielsen, Bone **35** 583 (2004).
[16] G. Boivin, P. Deloffre, B. Perrat, G. Panczer, M. Boudeulle, Y. Mauras, P. Allain, Y. Tsouderos, P. J. Meunier, J. Bone Miner. Res. **11** 1302 (1996).
[17] S. Yamada, T. Nakamura, T. Kokubo, M. Oka, T. Yamamuro, J. Biomed. Mater. Res. - Part A. **28** 1357 (1994).

[18] P. J. Meunier, C. Roux, E. Seeman, S. Ortolani, J. E. Badurski, T. D. Spector, J. Cannata, A. Balogh, E. M. Lemmel, S. Pors-Nielsen, R. Rizzoli, H. K. Genant, J. Y. Reginster, N. Engl. J. Med. **350** 459 (2004).
[19] D. Farlay, G. Boivin, G. Panczer, A. Lalande, P. J. Meunier, J. Bone Miner. Res. **20** 1569 (2005).
[20] A. Antonakos, E. Liarokapis, T. Leventouri, Biomaterials **28** 3043 (2007).
[21] S. Koutsopoulos, J. Biomed. Mater. Res. **62** 600 (2002).
[22] H. Ou-Yang, E. P. Paschalis, A. L. Boskey, R. Mendelsohn, Biopolymers **57** 129 (2000).
[23] S. Zou, J. Huang, S. Best, W. Bonfield, J. Mater. Sci.-Mater. Med. **16** 1143 (2005).
[24] G. Penel, G. Leroy, C. Rey, E. Bres, Calcif. Tissue Int. **63** 475 (1998).
[25] J. A. Gordon, C. E. Tye, A. V. Sampaio, T. M. Underhill, G. K. Hunter, H. A. Goldberg, Bone **41** 462 (2007).
[26] R. Filmon, M. F. Baslé, A. Barbier, D. Chappard, J. Biomater. Sci. Polym. Ed. **11** 849 (2000).
[27] H. Libouban, R. Filmon, A. Mauréac, M. F. Baslé, D. Chappard, J. Raman Spectrosc. **40** 1234 (2009).
[28] S. G. Dahl, P. Allain, P. J. Marie, Y. Mauras, G. Boivin, P. Ammann, Y. Tsouderos, P. D. Delmas, C. Christiansen, Bone **28** 446 (2001).
[29] P. J. Marie, P. Ammann, G. Boivin, C. Rey, Calcif. Tissue Int. **69** 121 (2001).
[30] X. Geng, L. Liu, J. Jiang, S. H. Yu, Crystal Growth Design **10** 3448 (2010).
[31] J. Christoffersen, M. R. Christoffersen, N. Kolthoff, O. Barenholdt, Bone **20** 47 (1997).
[32] P. Roschger, I. Manjubala, N. Zoeger, F. Meirer, R. Simon, C. Li, N. Fratzl-Zelman, B. M. Misof, E. P. Paschalis, C. Streli, P. Fratzl, K. Klaushofer, J. Bone Miner. Res. **25** 891 (2010).
[33] Z. Y. Li, W. M. Lam, C. Yang, B. Xu, G. X. Ni, S. A. Abbah, K. M. Cheung, K. D. Luk, W. W. Lu, Biomaterials **28** 1452 (2007).
[34] P. Ammann, V. Shen, B. Robin, Y. Mauras, J. P. Bonjour, R. Rizzoli, J. Bone Miner. Res. **19** 2012 (2004).
[35] B. Slat, K. Kostial, G. E. Harrison, Health Phys. **21** 811 (1971).
[36] C. Li, O. Paris, S. Siegel, P. Roschger, E. P. Paschalis, K. Klaushofer, P. Fratzl, J. Bone Miner. Res. **25** 968 (2010).
[37] M. I. Kay, R. A. Young, A. S. Posner, Nature **204** 1050 (1964).
[38] L. Granasy, T. Pusztai, T. Borzsonyi, J. A. Warren, J. F. Douglas, Nat. Mater. **3** 645 (2004).